# Adaptive Measurement Matrix Design in Compressed Sensing Based Direction of Arrival Estimation

*Berkan Kılıç[1,2], Alper Güngör[1,2], Mert Kalfa[1,2], Orhan Arıkan[1]*
[1]Department of Electrical and Electronics Engineering, Bilkent University, Ankara, Turkey
[2]ASELSAN Research Center, ASELSAN Inc., Ankara, Turkey
{bekilic, alpergungor, mkalfa}@aselsan.com.tr, oarikan@ee.bilkent.edu.tr

***Abstract*— Design of measurement matrices is an important aspect of compressed sensing (CS) based direction of arrival (DoA) applications that enables reduction in the analog channels to be processed in sparse target environments. Here, a novel measurement matrix design methodology for CS based DoA estimation is proposed and its superior performance over alternative measurement matrix design methodologies is demonstrated. The proposed method uses prior probability distribution of the targets to improve performance. Compared to the state-of-the-art techniques, it is quantitatively demonstrated that the proposed measurement matrix design approach enables significant reduction in the number of analog channels to be processed and adapts to a priori information on the target scene.**

***Keywords—Direction of arrival estimation, compressed sensing, measurement matrix design***

## I. Introduction

Direction of arrival (DoA) estimation is an important research topic with wide ranging applications including radar, electronic warfare systems, and wireless communications [1]. Historically, there is a progression towards techniques that exploit the signal structure to provide higher resolution of sources or targets beyond what is possible with a conventional beamformer [2], [3]. By using covariance matrix of the received data, Capon's beamformer [2] and Multiple Signal Classification (MUSIC) [3] techniques can resolve targets with narrow angular spacing. For acceptable performance, these methods require a number of snapshots for an accurate estimation of the covariance matrix. However, because of rank deficiency in the estimated covariance matrix, these approaches have challenges when the received signals from different directions of arrival (DoAs) are correlated, possibly due to multipath effects.

Development of compressed sensing (CS) based array signal processing techniques enabled DoA estimation with as few as a single snapshot and even for correlated sources [4]–[7]. Orthogonal Matching Pursuit (OMP) [8], Least Absolute Shrinkage and Selection Operator (LASSO) [9], Basis Pursuit Denoising (BPDN) [10] are among sparsity promoting algorithms that were successfully applied to the DoA applications [11]. Sparse DoA estimation techniques can also provide unambiguous results on compressed measurements rather than the measurements of each sensor. In a sensor array, these techniques can operate on digitized samples of linearly combined analog sensor outputs, equivalently performing a multiplication by a measurement matrix. Therefore, it is possible to perform reliable DoA estimation by using far fewer number of processing channels than the number of sensors in the sensor array. This creates an advantage in terms of size, weight, power, and cost (SWaP-C) of the sensor array system.

This work was supported in part by Turkish Scientific and Technological Research Council (TÜBİTAK) under the project CoSAMS-116E006

Choice of the measurement matrix has a significant effect on the reconstruction performance. Typically, a random Gaussian (RG) matrix is used as a measurement matrix for linear combination in CS literature [7]. There are studies in the literature using alternative measurement matrix design methods to surpass the performance provided by an RG matrix [12]–[19]. When a reasonably good prior estimate for the probability distribution of the source locations is available, a measurement matrix that exploits this prior information can be designed [16]–[18]. In this study, we propose a novel measurement matrix design technique that enables highly reduced number of channels as well as adapting to the prior information on the target scene. The proposed method is demonstrated and validated through a set of Monte Carlo simulations by using a uniform and linear array (ULA) with isotropic sensors. However, use of the proposed method is not limited to ULAs and can be easily adapted to an arbitrary array structure. Furthermore, we provide explanations on the theoretical limits of some common methods in the literature.

The rest of this paper is organized as follows. In Section II, DoA estimation with measurement matrices and compressed sensing is explained. The proposed measurement matrix design approach with its existing alternatives are given in Section III. Numerical results demonstrating superior performance of the proposed technique are presented in Section IV. Concluding remarks are given in Section V.

In the remainder of the manuscript, uppercase bold characters denote matrices and lowercase bold characters denote vectors, constants are denoted by uppercase or lowercase letters. $\ell_1$, $\ell_2$, and Frobenius norms are denoted by $\|\boldsymbol{x}\|_1$, $\|\boldsymbol{x}\|_2$, and $\|\boldsymbol{X}\|_\mathrm{F}$. $\boldsymbol{X}^\mathrm{T}$ and $\boldsymbol{X}^\mathrm{H}$ denote the transpose and the conjugate transpose of $\boldsymbol{X}$. tr() denotes trace and E{} denotes expectation.

## II. Direction of Arrival Estimation of Narrowband Sources by Sensor Arrays

Received signal $\boldsymbol{x}[k]$ by a sensor array at time $k$ for a set of narrowband sources with wavelength $\lambda$ located in the far-field of a sensor array can be written as

$$\boldsymbol{x}[k] = \boldsymbol{A}\boldsymbol{s}[k] + \boldsymbol{n}[k], \tag{1}$$

where $\boldsymbol{A} \in \mathbb{C}^{M\times L}$ is the array dictionary of $M$ sensors over a grid of $\theta_i$'s for $1 \le i \le L$, and $\boldsymbol{s} \in \mathbb{C}^{L\times 1}$ is the sparse source vector. Specifically, $\boldsymbol{A} = \frac{1}{\sqrt{M}}[\boldsymbol{a}(\theta_1)\ \boldsymbol{a}(\theta_2)\ \dots\ \boldsymbol{a}(\theta_L)]$ and $\boldsymbol{a}(\theta)$ denotes the response of the sensor array to a source at $\theta$ where $\omega(\theta) = \frac{2\pi d}{\lambda}\cos(\theta)$. For a ULA with isotropic sensors, $\boldsymbol{a}(\theta) = \left[1\ e^{j\omega(\theta)}\ \dots\ e^{j(M-1)\omega(\theta)}\right]^\mathrm{T}$. Conventionally, the normalization factor $1/\sqrt{M}$ is introduced so that the columns of $\boldsymbol{A}$ are unit-norm which is not crucial for DoA estimation in general. If $K$ sources were located exactly on the chosen grid

points, $\boldsymbol{s}$ would be $K$-sparse with only $K$ non-zero entries. Note that in the simulations, sources are generated on a continuous $\omega(\theta)$ domain to have a more objective assessment of the performance. Finally, $\boldsymbol{n} \in \mathbb{C}^{M\times 1}$ is an additive complex white Gaussian noise with standard deviation $\sigma$ and mean $\mathbf{0}$, i.e., $\boldsymbol{n}\sim N_C(\mathbf{0}, \sigma^2\boldsymbol{I}_M)$.

By using a measurement matrix $\boldsymbol{\Phi} \in \mathbb{C}^{m\times M}$, which can be realized in hardware with phase shifters, low noise amplifiers, and attenuators; compressed array outputs or measurements $\boldsymbol{y}$ can be obtained as

$$\boldsymbol{y} = \boldsymbol{\Phi A s} + \boldsymbol{\Phi n}. \tag{2}$$

In this form, $\boldsymbol{\Phi n}$ might not be a white Gaussian noise. By using a whitening matrix $\boldsymbol{W}$, we can whiten the obtained measurements as

$$\boldsymbol{Wy} = \boldsymbol{W\Phi A s} + \boldsymbol{W\Phi n}, \tag{3}$$

where $\boldsymbol{W\Phi n}\sim N_C(\mathbf{0}, \sigma^2\boldsymbol{I}_m)$. For this purpose, $\boldsymbol{W}$ can be chosen as $\boldsymbol{\Sigma}^{-\frac{1}{2}}\boldsymbol{U}^{\mathrm{H}}$ where $\boldsymbol{\Sigma}$ is the diagonal matrix of singular values and $\boldsymbol{U}$ is a unitary matrix of singular vectors of $\boldsymbol{\Phi\Phi}^{\mathrm{H}}$. An approximate sparse solution for $\boldsymbol{s}$ can be obtained as the solution to the following optimization problem [9], [10], which can be solved, e.g., by using the solver SPGL1 [20]:

$$\hat{\boldsymbol{s}} = \arg\min_{\boldsymbol{s}} \|\boldsymbol{s}\|_1$$
$$s.t. \|\boldsymbol{Wy} - \boldsymbol{W\Phi A s}\|_2^2 \le \beta^2, \tag{4}$$

where $\beta$ is chosen based on the noise statistics of the environment. Since $\boldsymbol{W}$ is chosen such that $\sigma^2\boldsymbol{W\Phi\Phi}^H\boldsymbol{W}^H = \sigma^2\boldsymbol{I}_m$, the residual error $\boldsymbol{Wy} - \boldsymbol{W\Phi A s}$ of the optimal solution of (4) is expected to be $\mathrm{E}\{\sigma^2\boldsymbol{W\Phi\Phi}^H\boldsymbol{W}^H\} = tr(\sigma^2\boldsymbol{I}_m) = \sigma^2 m$. So, $\beta^2 \cong \sigma^2 m$ is an appropriate choice independently of the designed measurement matrix $\boldsymbol{\Phi}$. Choice of $\beta$ is of crucial importance for an unbiased comparison between different $\boldsymbol{\Phi}$'s.

## III. Measurement Matrix Design in DoA Estimation

In the absence of prior information, $\boldsymbol{\Phi}$ in (2) is generally chosen to be an RG matrix since it satisfies the Restricted Isometry Property (RIP) with high probability [7]. Other alternative approaches have been proposed for the design of the measurement matrices [12]–[19], in particular for DoA applications [16]–[19]. Coherence minimization is a commonly used design rule for $\boldsymbol{\Phi}$ [12]. $L$ is typically larger than $M$, therefore; mutual coherence of $\boldsymbol{\Phi A}$ must be larger than zero. Since it is not possible to achieve zero mutual coherence for $\boldsymbol{\Phi A}$, it is well-known to formulate an optimization problem for the design of the measurement matrix $\boldsymbol{\Phi}$ as in [13]–[15], [19]:

$$\hat{\boldsymbol{\Phi}} = \arg\min_{\boldsymbol{\Phi}} \|(\boldsymbol{\Phi A})^{\mathrm{H}}(\boldsymbol{\Phi A}) - \boldsymbol{T}\|_{\mathrm{F}}^2, \tag{5}$$

where $\boldsymbol{T}$ denotes a target Gram matrix for $\boldsymbol{\Phi A}$. There are studies that choose $\boldsymbol{T}$ as an identity matrix implying no correlation between the different columns of $\boldsymbol{\Phi A}$ [13], [14]. In [19], $\boldsymbol{T} = \boldsymbol{A}^{\mathrm{H}}\boldsymbol{A}$ choice which is the case when $\boldsymbol{\Phi} = \boldsymbol{I}_M$ implying no reduction in the number of processing channels is proposed. However, in this case, the optimal solution becomes only selecting $m$ outputs of the $M$ sensors for $\boldsymbol{AA}^{\mathrm{H}} = C\boldsymbol{I}_M$ where $C$ is a constant, which is the investigated case in [19]. Therefore, $\boldsymbol{T} = \boldsymbol{A}^{\mathrm{H}}\boldsymbol{A}$ choice does not lead us to a desirable measurement matrix that compresses the available analog measurements. To show that, when $\boldsymbol{AA}^{\mathrm{H}} = C\boldsymbol{I}_M$ we can rewrite (5) as in [19]

$$\hat{\boldsymbol{\Phi}} = \arg\min_{\boldsymbol{\Phi}} \|\boldsymbol{\Phi}^{\mathrm{H}}\boldsymbol{\Phi} - \boldsymbol{ATA}^{\mathrm{H}}\|_{\mathrm{F}}^2. \tag{6}$$

If $\boldsymbol{T} = \boldsymbol{A}^{\mathrm{H}}\boldsymbol{A}$ in (6), we get

$$\hat{\boldsymbol{\Phi}} = \arg\min_{\boldsymbol{\Phi}} \|\boldsymbol{\Phi}^{\mathrm{H}}\boldsymbol{\Phi} - \boldsymbol{AA}^{\mathrm{H}}\boldsymbol{AA}^{\mathrm{H}}\|_{\mathrm{F}}^2. \tag{7}$$

Since $\boldsymbol{AA}^{\mathrm{H}} = C\boldsymbol{I}_M$, (7) becomes

$$\hat{\boldsymbol{\Phi}} = \arg\min_{\boldsymbol{\Phi}} \|\boldsymbol{\Phi}^{\mathrm{H}}\boldsymbol{\Phi} - C^2\boldsymbol{I}_M\|_{\mathrm{F}}^2, \tag{8}$$

where a solution is $\hat{\boldsymbol{\Phi}} = C[\boldsymbol{I}_m\ \mathbf{0}]$ which implies that only $m$ of the $M$ sensors should be used with no further scaling and phase shifting. This is equivalent to an uncompressed CS based DoA system with $m$ sensors, which loses information from the remaining $M - m$ sensors.

There are also studies suggesting use of equiangular tight frame (ETF) criterion [21] for $\boldsymbol{T}$ design [15]. ETF design is commonly used in CS literature to achieve Gram matrices having low coherence. If the matrix $\boldsymbol{\Phi A}$ is an ETF, its Gram matrix $\boldsymbol{G} := (\boldsymbol{\Phi A})^{\mathrm{H}}(\boldsymbol{\Phi A})$ must have the following structure:

$$G_{ij} = \begin{Bmatrix} \pm\mu_{Welch}, if\ i \ne j \\ 1, otherwise \end{Bmatrix}, \tag{9}$$

where $\mu_{Welch}$ is the minimum achievable mutual coherence by $\boldsymbol{\Phi A}$ and calculated as $\mu_{Welch} = \sqrt{\frac{L-m}{m(L-1)}}$ [22]. Note that the condition in (9) is not sufficient in itself for being an ETF [21]. There are also studies where $\boldsymbol{T}$ is chosen based on the probability distribution of the target DoAs. For example in [17], the diagonal entries of $\boldsymbol{T}$ are chosen based on the probability distribution of the target DoAs.

In this study, we propose a novel method of designing $\boldsymbol{T}$ by exploiting prior probability mass function (PMF) of the target DoAs. In the initial phase of target surveillance, prior target PMF is typically chosen as a uniform PMF. However, following detection and tracking of the targets, prior target PMFs highly deviate from the uniform PMF and shows accumulation around the predicted target positions provided by a tracker system. The targets for which we have prior information are called as the "tracked targets" in this study. In the design of the measurement matrix, emergence of new targets along with the tracked targets should also be considered. We will call the new targets in the scene as the "emerging targets". Here we propose the following mixture prior PMF for the overall target scene in the presence of $Q$ tracked targets with known PMFs:

$$p(\omega_i) = \sum_{q=1}^{Q} \alpha_q p_q(\omega_i) + \frac{(1-P_t)}{L}, 1 \le i \le L, \tag{10}$$

where $p_q(\omega_i)$ is the PMF of the $q^{th}$ tracked target on the grid point $\omega_i$ and the weights $\alpha_q > 0$ are chosen such that $\sum_{q=1}^{Q}\alpha_q = P_t \le 1$. This form of $p(\omega_i)$ combines the PMFs of the tracked targets and assigns a uniform prior for the potentially emerging targets. Based on the recent $\omega$ of the emerging targets, $P_t$ can be adjusted. If fewer targets are expected to emerge, $P_t$ should be increased; otherwise, decreased. Also, relative mixing weights $\alpha_q$'s of the tracked targets can be chosen to be proportional to their importance levels. In the proposed measurement matrix design approach, we propose the following $\boldsymbol{T}$ matrix to be used in (5):

$$T_{ij} = \begin{cases} cp(\omega_i), if\ i = j \\ \dfrac{\left|\boldsymbol{a}(\omega_i)^{\mathrm{H}}\boldsymbol{a}(\omega_j)\right|}{M}, if\ i \ne j \end{cases}, 1 \le i,j \le L, \tag{11}$$

where $\frac{1}{M}$ is a normalization factor and $c = \frac{1}{\min_i p(\omega_i)}$ provided that $\min_i p(\omega_i) \ne 0$. When $p(\omega_i) = 0$ or very close to 0 for

some $i$, we can set a small number, like $10^{-8}$, as the threshold for numerical stability. In the absence of the tracked targets, $\boldsymbol{T}$ becomes

$$T_{ij} = \frac{\left|\boldsymbol{a}(\omega_i)^{\mathrm{H}}\boldsymbol{a}(\omega_j)\right|}{M}, 1 \le i,j \le L. \quad (12)$$

In the remainder of this manuscript, we will call the design criterion given in (11) as the proposed design. It should be noted that the design criterion given in (12) is different from $\boldsymbol{T} = \boldsymbol{A}^{\mathrm{H}}\boldsymbol{A}$ choice which is shown to be severely limiting for a CS based DoA system.

Equation (5) has a closed form solution when $\boldsymbol{T}$ is a Hermitian matrix. Since $\boldsymbol{T}$ is the target matrix for $(\boldsymbol{\Phi A})^{\mathrm{H}}(\boldsymbol{\Phi A})$, it should always be Hermitian. Related derivation is studied in [19] and an expression was found for the case $\boldsymbol{A}\boldsymbol{A}^{\mathrm{H}} = C\boldsymbol{I}_M$. Restricting $\boldsymbol{A}$ such that it satisfies $\boldsymbol{A}\boldsymbol{A}^{\mathrm{H}} = C\boldsymbol{I}_M$ causes two important restrictions. First, the design works only for the case of isotropic ULAs with no mutual coupling effect and so on. Second, the grid selection can be done only by selecting angular grid points $\theta_i$'s such that they have uniformly spaced $\omega(\theta_i) = \frac{2\pi d}{\lambda}\cos(\theta_i)$ values. Note that the proposed approach can be extended to any array structure with an arbitrary grid. Also, any linear effect on $\boldsymbol{A}$ can be considered since the derivation is valid for an arbitrary matrix $\boldsymbol{A}$. To obtain the closed form solution of (5), we use (economy size) SVD of $\boldsymbol{A} = \boldsymbol{U}_A\boldsymbol{\Sigma}_A\boldsymbol{V}_A^{\mathrm{H}}$ where $\boldsymbol{U}_A^{\mathrm{H}}\boldsymbol{U}_A = \boldsymbol{U}_A\boldsymbol{U}_A^{\mathrm{H}} = \boldsymbol{I}_M$ and $\boldsymbol{V}_A^{\mathrm{H}}\boldsymbol{V}_A = \boldsymbol{I}_M$. Note that $\boldsymbol{V}_A\boldsymbol{V}_A^{\mathrm{H}} \neq \boldsymbol{I}_L$ and $\boldsymbol{\Sigma}_A$ is square. Writing $\boldsymbol{A} = \boldsymbol{U}_A\boldsymbol{\Sigma}_A\boldsymbol{V}_A^{\mathrm{H}}$, the problem becomes:

$$\hat{\boldsymbol{\Phi}} = \arg\min_{\boldsymbol{\Phi}} \left\| \boldsymbol{V}_A\boldsymbol{\Sigma}_A^{\mathrm{H}}\boldsymbol{U}_A^{\mathrm{H}}\boldsymbol{\Phi}^{\mathrm{H}}\boldsymbol{\Phi}\boldsymbol{U}_A\boldsymbol{\Sigma}_A\boldsymbol{V}_A^{\mathrm{H}} - \boldsymbol{T} \right\|_{\mathrm{F}}^2. \quad (13)$$

Defining $\boldsymbol{\Psi} \equiv \boldsymbol{\Phi}\boldsymbol{U}_A\boldsymbol{\Sigma}_A$, we can solve the following optimization problem since the invertible term $\boldsymbol{U}_A\boldsymbol{\Sigma}_A$ does not depend on $\boldsymbol{\Phi}$:

$$\hat{\boldsymbol{\Psi}} = \arg\min_{\boldsymbol{\Psi}} \left\| \boldsymbol{V}_A\boldsymbol{\Psi}^{\mathrm{H}}\boldsymbol{\Psi}\boldsymbol{V}_A^{\mathrm{H}} - \boldsymbol{T} \right\|_{\mathrm{F}}^2. \quad (14)$$

The Frobenius norm expression can be written as:

$$\left\| \boldsymbol{V}_A\boldsymbol{\Psi}^{\mathrm{H}}\boldsymbol{\Psi}\boldsymbol{V}_A^{\mathrm{H}} - \boldsymbol{T} \right\|_{\mathrm{F}}^2 =$$

$$\mathrm{tr}\left( (\boldsymbol{V}_A\boldsymbol{\Psi}^{\mathrm{H}}\boldsymbol{\Psi}\boldsymbol{V}_A^{\mathrm{H}} - \boldsymbol{T})(\boldsymbol{V}_A\boldsymbol{\Psi}^{\mathrm{H}}\boldsymbol{\Psi}\boldsymbol{V}_A^{\mathrm{H}} - \boldsymbol{T})^{\mathrm{H}} \right). \quad (15)$$

Using linearity and cyclic property of trace, we get:

$$\mathrm{tr}\left( (\boldsymbol{V}_A\boldsymbol{\Psi}^{\mathrm{H}}\boldsymbol{\Psi}\boldsymbol{V}_A^{\mathrm{H}} - \boldsymbol{T})(\boldsymbol{V}_A\boldsymbol{\Psi}^{\mathrm{H}}\boldsymbol{\Psi}\boldsymbol{V}_A^{\mathrm{H}} - \boldsymbol{T})^{\mathrm{H}} \right) =$$

$$\mathrm{tr}(\boldsymbol{\Psi}^{\mathrm{H}}\boldsymbol{\Psi}\boldsymbol{\Psi}^{\mathrm{H}}\boldsymbol{\Psi}) - 2\mathrm{tr}(\boldsymbol{\Psi}^{\mathrm{H}}\boldsymbol{\Psi}\boldsymbol{V}_A^{\mathrm{H}}\boldsymbol{T}\boldsymbol{V}_A) + \mathrm{tr}(\boldsymbol{T}\boldsymbol{T}^{\mathrm{H}}). \quad (16)$$

Calling the terms that do not depend on $\boldsymbol{\Psi}$ as the constant $D$ and observing that the trace terms in (16) can be written as $\left\| \boldsymbol{\Psi}^{\mathrm{H}}\boldsymbol{\Psi} - \boldsymbol{V}_A^{\mathrm{H}}\boldsymbol{T}\boldsymbol{V}_A \right\|_{\mathrm{F}}^2 + D$, (14) reduces to:

$$\hat{\boldsymbol{\Psi}} = \arg\min_{\boldsymbol{\Psi}} \left\| \boldsymbol{\Psi}^{\mathrm{H}}\boldsymbol{\Psi} - \boldsymbol{V}_A^{\mathrm{H}}\boldsymbol{T}\boldsymbol{V}_A \right\|_{\mathrm{F}}^2. \quad (17)$$

Since $\boldsymbol{\Psi}^{\mathrm{H}}\boldsymbol{\Psi}$ has rank $m$, by Eckart-Young-Mirsky Matrix Approximation Theorem [23], [24], the optimal choice of $\boldsymbol{\Psi}^{\mathrm{H}}\boldsymbol{\Psi}$ is the best rank-$m$ approximation of $\boldsymbol{V}_A^{\mathrm{H}}\boldsymbol{T}\boldsymbol{V}_A$. We call $\boldsymbol{Z} = \boldsymbol{V}_A^{\mathrm{H}}\boldsymbol{T}\boldsymbol{V}_A = \boldsymbol{U}_Z\boldsymbol{\Sigma}_Z\boldsymbol{U}_Z^{\mathrm{H}}$, which is a Hermitian matrix since $\boldsymbol{T}$ is Hermitian. Finally, we form rank-$m$ reduced form of $\boldsymbol{Z}$ by taking the first $m$ columns of $\boldsymbol{U}_Z$, the first $m$ columns and the first $m$ rows of $\boldsymbol{\Sigma}_Z$ and obtain the optimal $\boldsymbol{\Psi}$ matrix as

$$\hat{\boldsymbol{\Psi}} = \sqrt{\boldsymbol{\Sigma}_{Z_m}}\,\boldsymbol{U}_{Z_m}^{\mathrm{H}}. \quad (18)$$

Since $\hat{\boldsymbol{\Psi}} = \hat{\boldsymbol{\Phi}}\boldsymbol{U}_A\boldsymbol{\Sigma}_A$ and both $\boldsymbol{U}_A$ and $\boldsymbol{\Sigma}_A$ are invertible,

$$\hat{\boldsymbol{\Phi}} = \hat{\boldsymbol{\Psi}}\boldsymbol{\Sigma}_{\mathrm{A}}^{-1}\boldsymbol{U}_A^{\mathrm{H}}. \quad (19)$$

Equation (19) provides a closed form solution for the optimal measurement matrix based on the criterion in (5) for an arbitrary $\boldsymbol{A}$.

In Section IV, we will show superior performance of the proposed method over some methods studied in the literature which we briefly mention in this section. $\boldsymbol{T} = \boldsymbol{I}_L$ will be named as the Identity Matrix Design (IMD). Using ETF criterion, we can form the following target Gram matrix:

$$T_{ij} = \begin{cases} 1, & if\ i = j \\ \pm\mu_{welch}, & if\ i \neq j \end{cases}, 1 \le i,j \le L, \quad (20)$$

which we will call as the ETF Design (ETFD). In [17], an adaptive $\boldsymbol{T}$ design is proposed as

$$T_{ij} = \begin{cases} 1, if\ i = j \text{ and } \omega_i \in \Omega_H \\ 0, \text{otherwise} \end{cases}, 1 \le i,j \le L, \quad (21)$$

where $\Omega_H$ denotes the set of $\omega$ values of the tracked targets. In our simulations, (21) will be named as Ibrahim's Design (ID). For visualization, we will illustrate $\boldsymbol{T}$ designs for ID and the proposed design for a simple scenario. Note that the proposed design given in (11) has diagonal entries $cp(\omega_i)$ for $1 \le i \le L$. However, ID in (21) consists of ones and zeros which are adjusted using the target probability distribution $p(\omega_i)$. To illustrate these different choices, assuming a target probability distribution as given in TABLE I:

TABLE I. TARGET PROFILE – FOR ILLUSTRATION

| | DoA Distribution |
|---|---|
| Target 1 | $N(-1.57, 0.0391^2)$ |
| Target 2 | $N(1.07, 0.0391^2)$ |

Both of the targets are designated as the tracked targets for which we have the probability distribution, for example, from previous snapshots. DoA of the first target is selected from a Gaussian DoA distribution with mean $\omega(\theta) = -1.57$ and the second target is selected from a Gaussian DoA distribution with mean $\omega(\theta) = 1.07$ (in radians). Both of these target distributions have a standard deviation of $2.5 \times 2/M = 0.0391$ radians where $2/M$ is approximately the half power beamwidth of a ULA separated by $\lambda/2$ distance between the adjacent sensors [25]. Note that since $\omega(\theta) = \frac{2\pi d}{\lambda}\cos(\theta)$, $\omega(\theta)$'s in TABLE I correspond to 120° and 70° respectively. Standard deviation is a measure of uncertainty in $\omega(\theta)$'s, for example, depending on the target speeds. Assigning $\alpha_1 = \alpha_2 = 0.025$ in (11), diagonal of $\boldsymbol{T}$ which is chosen with respect to the criteria given in (11) and (21) are plotted in Fig. 1:

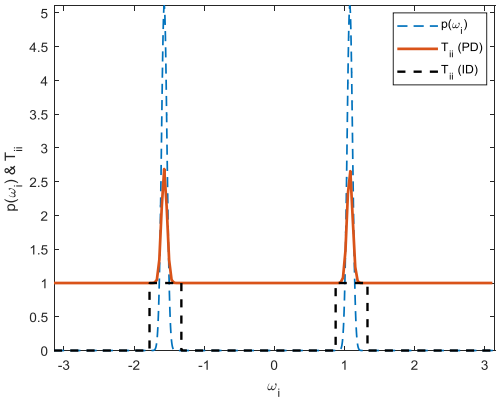


**Figure 1**: Diagonal elements of $\boldsymbol{T}$ when different design criteria are used. The term PD is used to denote Proposed Design.

As it is seen from Fig. 1, ID consists of ones and zeros. However, the proposed method does not include any zero entries in the diagonal in order not to miss any emerging target. Importance of this approach will be made clear in Section IV.

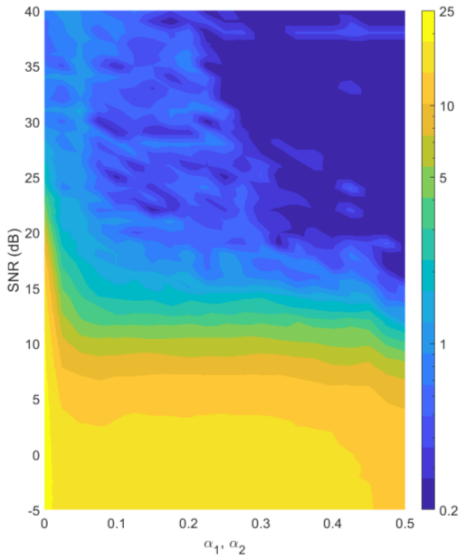


Fig. 2a

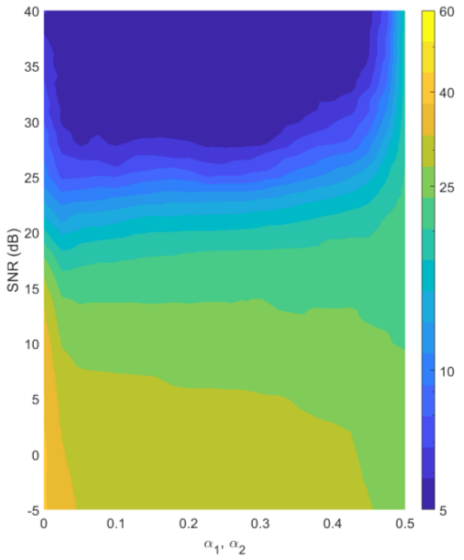


Fig. 2b

**Figure 2:** RMSE(°) plots with respect to different SNRs and different $\alpha_1, \alpha_2$ ($\alpha_1 = \alpha_2$) choices. Fig. 2a shows RMSE(°) values for the tracked targets and Fig. 2b shows RMSE(°) values for all (both tracked and emerging) targets. Readers should note that the color bars are differently scaled for Fig. 2a, and Fig. 2b.

## IV. Numerical Results

In this section, performance of the proposed measurement matrix design technique is investigated by using a ULA with $M = 128$ sensors spaced half-wavelength apart ($\lambda/2$) and reduced to $m = 16$ channels by using $\mathbf{\Phi} \in \mathbb{C}^{m \times M}$. Only a single snapshot is taken in all simulations and $L = 180$ grid points equally separating $\omega(\theta) = \frac{2\pi d}{\lambda}\cos(\theta)$ values are used. Signal-to-noise ratio (SNR) is defined as $SNR = SNR_e + 10\log_{10} M$ where $SNR_e$ is the $SNR$ at each sensor in the array, which is defined as $SNR_e \equiv 10\log_{10}(P_s/\sigma^2)$, where $P_s$ denoting the source power. In our simulations, all sources are assumed to be uncorrelated and broadcast with the same power. Note that the proposed method can also be used in a scenario with correlated sources. For the results given in TABLE III and IV; 250,000 Monte Carlo simulations are performed whereas for the results given in Fig. 2; 10,000 Monte Carlo simulations are performed each with independent DoA and noise realizations. We use an RMSE (root mean squared error) based performance evaluation criterion to evaluate the performance of the methods on the tracked targets and all (both emerging and tracked) targets separately. To achieve the given RMSE values, squared difference between each of the estimated and real DoA is computed in degree unit and averaged over $K_e$ targets and $N_{mc}$ Monte Carlo iterations. Let $\theta_{ki}$ and $\hat{\theta}_{ki}$ denote the real and estimated DoA angles for the $k'$th target in the $i'$th Monte Carlo iteration, then RMSE is computed as follows:

$$\text{RMSE} = \sqrt{\frac{1}{N_{mc}K_e}\sum_{n=1}^{N_{mc}}\sum_{k=1}^{K_e}\left(\hat{\theta}_{nk} - \theta_{nk}\right)^2}. \qquad (22)$$

Note that $K_e = Q$ when only tracked targets are evaluated and $K_e = K$ when all targets are evaluated.

In the simulation scenario, assuming that there is an emerging target in addition to the tracked targets given in TABLE I. The third "emerging" target is selected from a uniform distribution between $-0.9\pi$ and $0.9\pi$ (in radians). Parameters for such a case are summarized in TABLE II:

TABLE II. TARGET PROFILE FOR THE GIVEN SCENARIO

| | DoA Distribution |
|---|---|
| Target 1 | $N(-1.57, 0.0391^2)$ |
| Target 2 | $N(1.07, 0.0391^2)$ |
| Target 3 | $U(-0.9\pi, 0.9\pi)$ |

As explained before, placing scaled PMFs $cp(\omega_i)$ as the diagonal entries of $\boldsymbol{T}$ requires a single PMF expression as given in (10). Therefore, we should determine $\alpha_1$ and $\alpha_2$ appropriately. In Fig. 2, we provide the RMSE values for different $\alpha_1, \alpha_2$ choices and various SNRs for the given scenario. We set $\alpha_1 = \alpha_2$ such that both tracked targets are of equal importance. We used 1 dB step size for SNR and 0.025 step size for $\alpha_1, \alpha_2$. Since the final aim is to minimize error for both tracked and emerging targets, we see from Fig. 2b that for low SNRs, $\alpha_1 = \alpha_2 \cong 0.5$ is the best choice. Practically for low SNR regime, it may be desirable for the DoA system to focus on the tracked targets such that it does not miss them at the cost of catching the emerging targets which may not be possible due to the highly noisy environment. For middle SNRs, $\alpha_1 = \alpha_2 \cong 0.025$, which is a very small value, gives the lowest RMSE values. Intuition behind such a choice is that the DoA system can reliably find DoAs of the emerging targets at the mid-SNR regime. Therefore, system should also attach high importance on the emerging targets. For high SNR regime, all $\alpha_1, \alpha_2$ choices are reasonable except for the ones that are close to 0.50. The reason is that when $\alpha_1$ and $\alpha_2$ are chosen very high, DoA system misses the emerging targets since it attaches unnecessarily high importance on the tracked targets. From Fig. 2a, we see that high $\alpha_1, \alpha_2$ choices perform the best as expected since only the tracked targets are considered in Fig. 2a.

Naming PD1 as the proposed design when $\alpha_1 = \alpha_2 = 0$, PD2 when $\alpha_1 = \alpha_2 = 0.025$, PD3 when $\alpha_1 = \alpha_2 = 0.225$,

PD4 when $\alpha_1 = \alpha_2 = 0.50$ are chosen as PMF mixture weights, we get the following RMSE values:

TABLE III. RMSE(°) RESULTS FOR THE TRACKED TARGETS

| **Methods** | **SNR** | | | | | | | | | | |
|---|---|---|---|---|---|---|---|---|---|---|---|
| | *-5 dB* | *0 dB* | *5 dB* | *10 dB* | *15 dB* | *20 dB* | *25 dB* | *30 dB* | *35 dB* | *40 dB* | *45 dB* |
| *RG* | 24.42 | 24.44 | 24.36 | 23.84 | 22.33 | 18.64 | 13.07 | 9.35 | 7.94 | 7.48 | 7.28 |
| *IMD* | 24.88 | 24.87 | 24.60 | 23.85 | 22.05 | 18.43 | 13.02 | 9.12 | 7.64 | 7.21 | 6.94 |
| *ETFD* | 23.53 | 23.53 | 23.29 | 22.63 | 20.49 | 15.58 | 9.19 | 5.74 | 4.53 | 4.25 | 4.10 |
| *PD1* | 21.07 | 20.92 | 20.44 | 19.04 | 15.19 | 7.60 | 2.11 | 1.03 | 0.72 | 0.63 | 0.56 |
| *PD2* | 15.90 | 15.12 | 12.74 | 8.05 | 4.04 | 1.86 | 1.08 | 0.82 | 0.78 | 0.82 | 0.79 |
| *PD3* | 16.11 | 15.34 | 12.58 | 6.03 | 1.29 | 0.55 | 0.50 | 0.48 | 0.44 | 0.36 | 0.40 |
| *PD4* | **12.16** | **11.77** | **9.51** | **3.14** | **0.48** | **0.25** | **0.25** | **0.22** | **0.23** | 0.24 | **0.22** |
| *ID* | 12.85 | 12.52 | 10.12 | 3.64 | **0.48** | 0.30 | **0.25** | 0.23 | 0.24 | **0.22** | **0.22** |

TABLE IV. RMSE(°) RESULTS FOR ALL TARGETS

| **Methods** | **SNR** | | | | | | | | | | |
|---|---|---|---|---|---|---|---|---|---|---|---|
| | *-5 dB* | *0 dB* | *5 dB* | *10 dB* | *15 dB* | *20 dB* | *25 dB* | *30 dB* | *35 dB* | *40 dB* | *45 dB* |
| *RG* | 40.18 | 40.19 | 39.93 | 39.05 | 36.68 | 31.22 | 22.77 | 16.91 | 14.83 | 14.06 | 13.78 |
| *IMD* | 40.11 | 39.98 | 39.56 | 38.54 | 35.80 | 30.19 | 21.90 | 16.17 | 13.89 | 13.22 | 12.89 |
| *ETFD* | 39.35 | 39.38 | 38.99 | 38.04 | 35.18 | 28.40 | 18.45 | 12.62 | 10.67 | 10.10 | 9.75 |
| *PD1* | 38.85 | 38.48 | 37.70 | 35.41 | 29.61 | 18.21 | 10.17 | 8.01 | 6.63 | 5.76 | 5.18 |
| *PD2* | 33.09 | 32.34 | 30.66 | 27.26 | **22.26** | **14.51** | **7.86** | 5.84 | 5.41 | 5.32 | 5.05 |
| *PD3* | 30.47 | 29.88 | 28.28 | 25.41 | 22.75 | 17.81 | 8.47 | **4.88** | **4.43** | **4.39** | **4.39** |
| *PD4* | **26.25** | **26.04** | **25.21** | **23.47** | 22.73 | 21.80 | 20.49 | 19.18 | 18.61 | 18.57 | 18.68 |
| *ID* | 26.59 | 26.29 | 25.37 | 23.63 | 23.20 | 23.14 | 22.99 | 22.78 | 22.56 | 22.41 | 22.31 |

Smallest RMSE values for the corresponding SNRs are denoted by bold numbers. From TABLE III, we see that when $\alpha_1 = \alpha_2 = 0.50$ is used, PD4 performs very well for all SNRs as expected since the DoA system is designed only to focus on the tracked targets. TABLE IV shows that even if $\alpha_1 = \alpha_2 = 0.50$ choice works very well for the tracked targets, for all targets at high SNRs, $\alpha_1 = \alpha_2 = 0.50$ choice is not appropriate since the emerging targets are almost completely missed with that choice. Similar situation is observed for ID. ID works well for the tracked targets; however, it almost completely misses the emerging targets. An important advantage of our proposed method is the flexibility of being able to adjust the parameters depending on the target scene. Comparing all of the given methods, we see that the proposed design outperforms all other alternative methods at all SNRs except for the case of the tracked targets at SNR $= 40$ dB. In this case RMSE values for ID and PD4 are about the same where the difference is around $0.02°$.

## V. CONCLUSIONS

In this study, we proposed and demonstrated an adaptive measurement matrix design methodology for CS based DoA estimation. Performance improvement of the proposed measurement matrix design technique is demonstrated over many alternative measurement matrix design methodologies. The proposed design enables adjustment of the DoA system depending on the importance levels of the targets and their expected positions, SNR, etc.

As a future work, we will fully integrate a target tracker to the compressed array signal processor and provide prior information based on the tracker predictions. Furthermore, we will investigate concerns resulting from hardware implementations, for example, effect of sensitivity of the hardware components, antenna directivity, and mutual coupling between the antenna elements.

## REFERENCES


[1] H. Krim, and M. Viberg, "Two decades of array signal processing research: The parametric approach," *IEEE Signal Process. Mag*., vol. 13, July 1996.

[2] J. Capon, "High resolution frequency-wavenumber spectrum analysis," *Proc. IEEE*, vol. 57, pp. 1408–1418, Aug. 1969.

[3] R. Schmidt, "Multiple emitter location and signal parameter estimation, *IEEE Trans. Antennas Propagat*., vol. 34, no. 3, pp. 276–280, Mar. 1986.

[4] E. J. Candes, J. Romberg, and T. Tao, "Robust uncertainty principles: Exact signal reconstruction from highly incomplete frequency information," *IEEE Trans. Inform. Theory*, vol. 52, no. 2, pp. 489–509, Feb. 2006.

[5] D. Donoho, "Compressed sensing," *IEEE Trans. Inform. Theory*, vol. 52, no. 4, pp. 1289–1306, April 2006.

[6] E. J. Candes, and M. B. Wakin, "Compressive sampling," *IEEE Signal Process. Mag*., vol. 25, no. 2, pp. 21–30, March 2008.

[7] E. J. Candès, and T. Tao, "Near-optimal signal recovery from random projections: Universal encoding strategies?," *IEEE Trans. Inform. Theory*, vol. 52, no. 12, pp. 5406–5425, Dec. 2006.

[8] J. Tropp, and A. Gilbert, "Signal recovery from random measurements via orthogonal matching pursuit," *IEEE Trans. Inform. Theory*, vol. 53, no. 12, pp. 4655–4666, Dec. 2007.

[9] R. Tibshirani, "Regression shrinkage and selection via the lasso," *Journal of the Royal Statistical Society*, vol. 58, no. 1, pp. 267–288, 1996.

[10] S. S. Chen, D. L. Donoho, and M. A. Saunders, "Atomic decomposition by basis pursuit," *SIAM J. Sci. Comput*., vol. 20, no. 1, pp. 33–61, 1998.

[11] Z. Yang, J. Li, P. Stoica, and L. Xie, "Sparse methods for direction-of-arrival estimation," 2017, arXiv:1609.09596v2.

[12] M. Elad, "Optimized projections for compressed sensing," *IEEE Trans. Signal Process*., vol. 55, no. 12, pp. 5695–5701, Dec. 2007.

[13] J. M. Duarte-Carvajalino, and G. Sapiro, "Learning to sense sparse signals: simultaneous sensing matrix and sparsifying dictionary optimization," *IEEE Trans. Image Process.*, vol. 18, no. 7, pp. 1395–1408, 2009.

[14] V. Abolghasemi, S. Ferdowsi, B. Makkiabadi, and S. Sanei, "On optimization of the measurement matrix for compressive sensing," in *Proc. Eur. Signal Process. Conf*., Aalborg, Denmark, Aug. 2010, pp. 427–431.

[15] V. Abolghasemi, S. Ferdowsi, and S. Sanei, "A gradient-based alternating minimization approach for optimization of the measurement matrix in compressive sensing," *Signal Process*., vol. 92, pp. 999–1009, 2012.

[16] Y. Gu, Y. D. Zhang, and N. A. Goodman, "Optimized compressive sensing based direction-of-arrival estimation in massive MIMO," in *Proc. IEEE Int. Conf. Acoust., Speech, Signal Process*., New Orleans, LA, USA, Mar. 2017, pp. 3181–3185.

[17] M. Ibrahim, F. Roemer, and G. D. Galdo, "An adaptively focusing measurement design for compressed sensing based doa estimation," in *Proc. Eur. Signal Process. Conf.,* 2015, pp. 859–863.

[18] B. Özer, A. Lavrenko, S. Gezici, G. Del Galdo, and O. Arıkan, "Adaptive measurement matrix design for compressed doa estimation with sensor arrays," in *Proc. Asilomar Conf. Signals, Syst. Comput.*, 2015, pp. 1769–1773.

[19] M. Ibrahim, F. Roemer, and G. D. Galdo, "On the design of the measurement matrix for compressed sensing based DOA estimation," in *Proc. Int. Conf. Acoust., Speech, Signal Process*., Apr. 2015.

[20] E. van den Berg, and M. P. Friedlander, "SPGL1: A solver for large-scale sparse reconstruction," [Online]. Available: https://friedlander.io/spgl1

[21] M. Sustik, J. A. Tropp, I. S. Dhillon, R. W. Heath Jr., "On the existence of equiangular tight frames," *Linear Algebra and Its Appl.*, vol. 426, no. 2–3, pp. 619–635, 2007.

[22] L. R. Welch, "Lower bounds on the maximum cross correlation of signals," *IEEE Trans. Inform. Theory*, vol. 20, no. 3, pp. 397–399, May 1974.

[23] C. Eckart, and G. Young, "The approximation of one matrix by another of lower rank," *Psychometrika*, vol. 1, pp. 211-218, 1936.

[24] L. Mirsky, "Symmetric gauge functions and unitarily invariant norms," *Quart. J. Math*., vol. 11, no. 1, pp. 50–59, 1960.

[25] M. A. Richards, *Fundamentals of Radar Signal Processing*, New York, NY, USA: McGraw Hill, 2005.